Nuclear Instruments and Methods in Physics Research A 690 (2012) 96–101

Contents lists available at SciVerse ScienceDirect

Nuclear Instruments and Methods in Physics Research A

journal homepage: www.elsevier.com/locate/nima

Neutron detection in a high gamma-ray background with EJ-301 and EJ-309 liquid scintillators

L. Stevanato [a,*], D. Cester [a], G. Nebbia [b], G. Viesti [a]

[a] Dipartimento di Fisica ed Astronomia dell' Università di Padova, Fisica "Galileo Galilei", Via Marzolo 8, I-35131 Padova, Italy
[b] INFN Sezione di Padova, Via Marzolo 8, I-35131 Padova, Italy

ARTICLE INFO

Article history:
Received 20 April 2012
Received in revised form
1 June 2012
Accepted 19 June 2012
Available online 4 July 2012

Keywords:
Liquid scintillator
Digital signal processing

ABSTRACT

Using a fast digitizer, the neutron–gamma discrimination capability of the new liquid scintillator EJ-309 is compared with that obtained using standard EJ-301. Moreover the capability of both the scintillation detectors to identify a weak neutron source in a high gamma-ray background is demonstrated. The probability of neutron detection is $PD=95\%$ at 95% confidence level for a gamma-ray background corresponding to a dose rate of 100 μSv/h.

1. Introduction

Organic liquid scintillators are commonly employed for fast neutron detection thanks to their pulse shape discrimination (PSD) capability used to separate neutrons from the gamma-ray component of the radiation field (see for example [1]). Being the liquid scintillator a standard tool in basic research [2], such detectors have found a rather marginal use in Homeland Security applications since many operational contexts prohibit these liquids because of their toxicity and flammability. Moreover liquid scintillators detect neutron above a low energy threshold (usually few hundred keV) and exhibit a good gamma-ray efficiency so that such detectors are normally characterized by a modest gamma-ray rejection capability, a property that is required to identify weak neutron source in a strong gamma-ray background [3].

However, it has been recently pointed out that selecting the fast neutron energy region in the total neutron spectrum optimizes the signal-to-background ratio thus improving the detection of weak neutron sources [4]. New liquid scintillation materials have become recently available as the EJ-309 type [5], from Eljen Technology, which is characterized by low toxicity and high flash point (144 °C) compared to the more traditional EJ-301 (flash point 26 °C) which is equivalent to the well known NE-213.

The EJ-309 scintillator has been employed in pure and applied research works confirming a PSD capability well suited to perform neutron spectroscopy [6,7]. Moreover the gamma rejection capability of the EJ-309 was the subject of a recent study [8].

In this work we will study the possible application of liquid scintillator detectors in the field of Homeland Security with respect to neutron detection in an intense gamma-ray background.

2. Experimental details

The detectors studied in this work consist of 2 in. × 2 in. liquid scintillator cells coupled to an H1949-51 HAMAMATSU photomultiplier (PMT) through an EJ-560 silicon rubber interface.

The PMT anode signals were directly fed into a CAEN V1720 12 bit 250 MS/s Digitizer. The PMTs are operated at relatively low voltage ($HV=1600$ V), to avoid saturation effects in digitizing the pulses. Inside the V1720 card, Digital Pulse Processing (DPP) algorithms are implemented using FPGA, providing on-line for each event (a) a time stamp, (b) a complete integration of the signal, (c) a partial integration of the signal used for PSD and (d) the possibility of storing a selected part of the digitized signal. Consequently, in the V1720 card some parameters need to be tuned in order to optimize the PSD, once the "Long Gate" (i.e. the number of FADC bins used in the total pulse integration) is properly set. Such parameters are the "Short Gate" (i.e. the number of FADC bins used in the integration of the fast part of the pulse), the "Pre-Gate" (establishing the point before the crossing of the low energy threshold from which the integration is started) and the "Baseline Threshold" (i.e. the number of points used for the definition of the baseline level). In our experimental set-up the PSD parameter is then computed on-line as

* Corresponding author. Tel.: +39 0498275936.
E-mail address: luca.stevanato@pd.infn.it (L. Stevanato).

0168-9002/$ - see front matter © 2012 Elsevier B.V. All rights reserved.
http://dx.doi.org/10.1016/j.nima.2012.06.047

PSD=(Long Gate Integration − Short Gate Integration)/Long Gate Integration.

In order to characterize the neutron–gamma discrimination capability we used the Figure of Merit (FoM) obtained by analyzing the PSD distribution from a ^{252}Cf source. It is defined as $FoM=S/(\Gamma_e+\Gamma_p)$ where S is the difference between the two centroids of the neutron and gamma peaks and $(\Gamma_e+\Gamma_p)$ is the sum of the gamma and neutron full widths at half maximum [FWHM] [9]. The optimization of the DPP parameters has been performed empirically by maximizing the FoM corresponding to different sets of the DPP parameters. It is found that the optimized DPP parameters for the EJ-301 and EJ-309 detectors are identical: 70 and 17 bins for the Long and Short Gates, respectively, 10 bins for the Pre-gate and 4 bins for the Baseline Threshold (each bin is 4 ns wide). With the above parameters, each pulse is characterized by 70 samples and the V1720 Digitizers handles count rate up about 100 kHz without dead time.

Finally, the energy calibration of the scintillation light was established by using the procedure described in [10] based on the fit of the experimental pulse shape distribution by using the theoretical Compton scattering distribution with an empirical spreading width to account for the finite detector resolution. Samples of those spectra for a ^{22}Na radioactive source are reported in Fig. 1.

It is immediately evident from Fig. 1 that the spectra measured with the two scintillators are very similar. The calibration procedure allows one to obtain an estimate of the detector pulse height resolution by determining the spreading width σ needed to reproduce the Compton Edge structures (for more details see [10]). The energy resolution is defined as σ/L where L is the energy value of the Compton Edge. The energy resolution derived in this case for the two liquid scintillators is $\sigma/L=6.0\%$ for the Compton Edge of the 1275 keV gamma-ray ($\sigma/L=8.2\%$ for the Compton Edge of the 511 keV gamma-ray). This figure is slightly better with respect to those reported in [10] for a 2 in. × 2 in. EJ-228 plastic scintillator processed with standard NIM electronics.

Finally, the low energy detection threshold, as determined from the spectra in Fig. 1, results to be about 60 keV.

3. Pulse shape discrimination

The response of the different scintillators was studied using a weak ^{252}Cf source (0.7×10^4 neutron/s) placed at about 15 cm from the detector front face. Typical PSD versus energy scatter plots are shown in Fig. 2. In this representation the neutron and gamma regions can be separated by a cut at $PSD=0.09$ for the EJ-301 and $PSD=0.16$ for the EJ-309 for energies larger than 300 keV.

A number of PSD spectra have been produced by varying the low energy threshold and analyzed. Extracted *FoM* values are reported in Fig. 3 for the two detectors explored in this work as a function of the low energy threshold.

It is seen from Fig. 3 that the *FoM* increases, improving the discrimination, with the low energy threshold reaching values $FoM>1.5$ for thresholds of about 300 keV. This threshold value corresponds to about 1.5 MeV in proton energy by using the

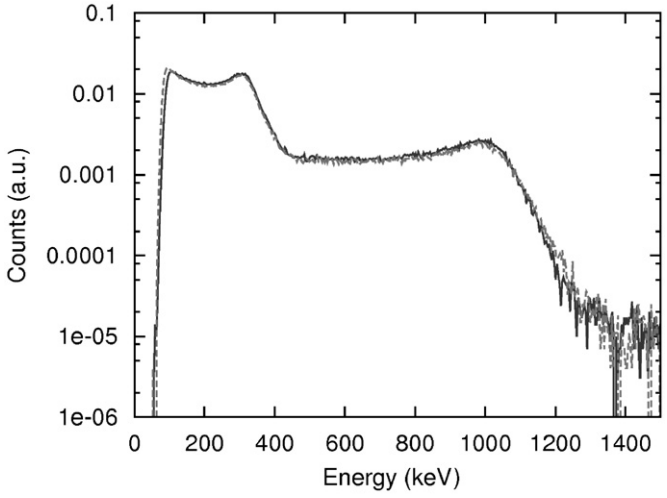

Fig. 1. Calibrated ^{22}Na pulse height distribution for the detectors studied in this work: EJ-301 full line, EJ-309 dashed line.

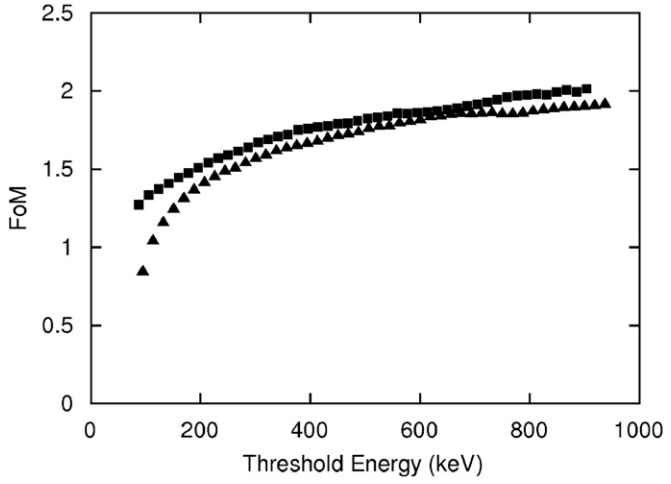

Fig. 3. Figure-of-Merit parameter (FoM) as a function of the low energy threshold for the detectors studied in this work. EJ-301 detected as squares and EJ-309 as triangles. The statistical uncertainties are within the point size.

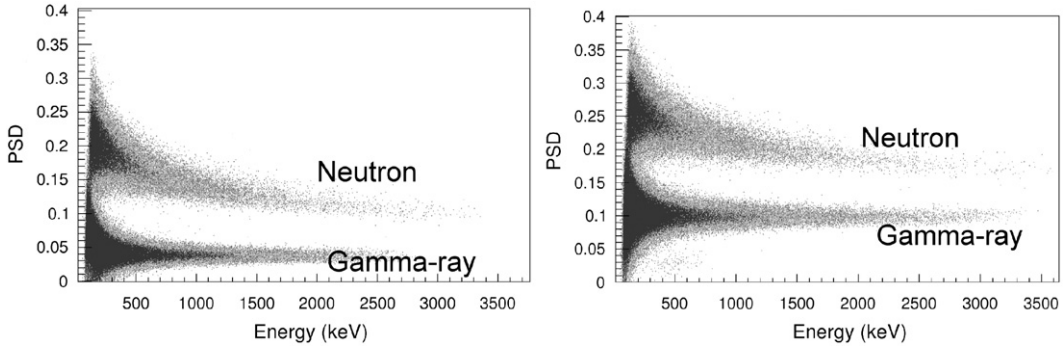

Fig. 2. Scatter plot PSD versus energy of a ^{252}Cf source measured with the EJ-301 detector (left) and EJ-309 (right).